Heliyon 9 (2023) e19149

Contents lists available at ScienceDirect

Heliyon

journal homepage: www.cell.com/heliyon

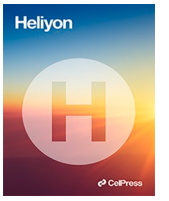

# Paeonol improves angiotensin II-induced cardiac hypertrophy by suppressing ferroptosis

Canzhang Liu [a], Xin Yi [a], Jie Yan [a], Qiang Liu [a], Teng Cao [a], Shuipeng Liu [b,*]

[a] Department I of Cardiovasology, North China University of Science and Technology Affiliated Hospital, Tangshan City, Hebei Province, 063000, PR China

[b] Department of Ultrasonic Medicine, North China University of Science and Technology Affiliated Hospital, Tangshan City, Hebei Province, 063000, PR China

ARTICLE INFO

*Keywords:*
Paeonol
Angiotensin II
Cardiac hypertrophy
Ferroptosis
xCT/GPX4

ABSTRACT

The aim of this study was to investigate the protective effect of paeonol (pae) on an angiotensin II (AngII)-induced cardiac hypertrophy mouse model. First, AngII mouse models were constructed and randomly grouped into the control (con), AngII, and AngII + Pae groups. Compared with that in the blank group, the surface area of myocardial cells in the AngII group increased significantly. In contrast to that in the AngII group, the cardiomyocyte surface area in the Pae group was significantly reduced. Ultrasound results showed that the myocardial function of mice in the AngII group was decreased compared with that in the Con group, while the myocardial function of mice in the Pae treatment was significantly improved. Moreover, the $Fe^{2+}$ and lipid peroxide levels of primary cardiomyocytes were significantly increased after treatment with AngII and were significantly decreased after the addition of Pae. Compared with those in the Con group, cristae were reduced and the outer membrane was lost in the myocardial tissues of the AngII group, and myocardial MDA, ROS, and $Fe^{2+}$ levels were increased. However, myocardial damage was significantly alleviated after Pae treatment, and myocardial MDA, ROS, and $Fe^{2+}$ levels were reduced. Moreover, in myocardial tissue, AngII reduced the protein levels of xCT and GPX4, while the levels of both xCT and GPX4 were increased after Pae treatment. In conclusion, Pae protected the hearts of AngII mice by upregulating the protein expression of xCT and GPX4 and resisting AngII-induced ferroptosis in cardiomyocytes.

## 1. Introduction

Myocardial hypertrophy and myocardial fibrosis often lead to heart failure, which is the end stage of various heart diseases and is a common cause of clinical death [1]. Several studies have shown that excessive activation of the renin-angiotensin (Ang)-aldosterone system (RAAS) plays a crucial role in myocardial fibrosis and cardiac hypertrophy [2–4]. RAAS activation increases Ang-converting enzyme activity, leading to increased conversion of Ang I to Ang II, resulting in elevated circulatory resistance and activation of the aldosterone system [2,3,5]. Although there are other neurohormones such as aldosterone, catechol amines and ET-1, Ang II is one of the major effectors and plays an important role in myocardial hypertrophy [3]. AngII stimulates cardiac fibroblast proliferation, collagen synthesis and matrix collagen deposition, inducing myocardial fibrosis [6]. Myocardial fibrosis is closely related to left

* Corresponding author.
*E-mail address:* Xinnei66696@163.com (S. Liu).

https://doi.org/10.1016/j.heliyon.2023.e19149
Received 20 March 2023; Received in revised form 26 July 2023; Accepted 14 August 2023
Available online 21 August 2023

ventricular hypertrophy and heart failure [7]. Therefore, we established an AngII-induced myocardial hypertrophy model in mice.

In addition to apoptosis, autophagy, and necrosis, ferroptosis is involved in heart failure [8]. Ferroptosis is an iron-dependent and nonapoptotic form of cell death characterized by oxidative damage resulting from the accumulation of lipid peroxides [9]. At the ultrastructural level, it typically exhibits mitochondrial abnormalities such as coalescence or swelling, increased membrane density, reduced or absent cristae, and rupture of the outer membrane [10]. Glutathione peroxidase 4 (GPX4) is a key protein that induces the onset of ferroptosis [11]. System Xc- (a cystine/glutamate antiporter system) is a heterodimer that includes a light chain (also called xCT or SLC7A11) and a heavy chain 4F2hc [12]. This protein takes in cystine in exchange for intracellular glutamate, which binds to glutamine and glycine to form glutathione (GSH) [12]. GSH is catalyzed by GPX4 to form a kinetic equilibrium with oxidized glutathione [13]. Inhibition of GPX4 and GSH synthesis initiates ferroptosis, and inhibition of cysteine uptake leads to the accumulation of lipid peroxides [13]. Many studies have shown that inhibiting ferroptosis in cardiomyocytes can prevent the development of cardiovascular disease [14–16]. Therefore, investigating the mechanism of ferroptosis prevention will provide a new target for heart failure prevention and treatment.

Paeonol (pae) is a small molecule phenolic compound that is a natural active substance with low toxicity [17]. Modern pharmacological studies have shown that pae has a wide range of pharmacological effects, such as antioxidant, anti-inflammatory, hypolipidemic and hypoglycemic effects [18–20]. Pae has been shown to reduce the inflammatory damage associated with atherosclerosis [21], but the protective effect of Pae on AngII-induced myocardial hypertrophy is unclear. In this study, we constructed in vivo and in vitro AngII-induced myocardial hypertrophy models and investigated whether Pae improved myocardial hypertrophy by inhibiting ferroptosis, thus exploring whether Pae was a possible therapeutic agent against myocardial hypertrophy.

## 2. Materials and methods

### 2.1. Animals

Twenty-four C57BL/6J mice (male, 6–8 weeks, 18–22 g, SiPeiFu Co., Beijing, China) were housed with a daily 12/12 h light/dark cycle at a room temperature of 22 ± 1 °C. The mice were provided free access to water and food. For anesthesia, 10% chloral hydrate (1 ml/100 g, Beijing Solarbio Science & Technology Co., Ltd., Beijing, China) was injected intraperitoneally. When the mice lost consciousness and responded to painful stimuli for approximately 5 min, anesthesia was successfully induced. The experimental mice were randomly divided into the sham group (n = 6) and AngII group (n = 18). The mice in the experimental group were weighed and subcutaneously injected with AngII continuously for 2 weeks at the required concentration for modeling, which was 1.4 mg/kg.day, with an output rate of 0.25 μl/h via an implantable capsule osmolarity pump (Alzet, USA). At the end of the treatment, systolic blood pressure was measured with a Kent Scientific CODA blood pressure recording system (KENT, USA). Elevated blood pressure predicted successful modeling in the AngII group. A previous study has indicated that Pae improves heart failure induced by transverse aortic constriction at a dose of at the doses of 25 mg/kg and 50 mg/kg or chronic heart failure induced by doxorubicin [22,23]. To compare the effects of higher dose of Pae, we chose 50 mg/kg and 100 mg/kg in the present study. The AngII group was then randomly divided into three groups (n = 6 for each group): the control group and low- and high-dose Pae groups [50 and 100 mg/(kg.d), L-Pae and H-Pae]. Pae was administered by gavage, and equal doses of saline were administered by gavage once daily for 8 weeks in each group. The study was approved by the Ethics Committee of North China University of Science and Technology.

### 2.2. Echocardiography (ECG) in mice

The mice were first anesthetized by an intraperitoneal injection of 10% chloral hydrate (1 ml/100 g) using a 1 ml syringe, followed by hair removal from the anterior thoracic region using a hair removal cream (Xiuzheng Co., Guangzhou, China) A small-animal high-resolution ultrasound system (VisualSonics, Japan) was used for ultrasound detection. The main measurements included left ventricular ejection fraction (LVEF), left ventricular internal dimension at end diastole/systole (LVIDd/LVIDs), left ventricular shortening (LVFS), and left ventricular posterior wall thickness at end diastole/systole (LVPWd/LVPWs), and the average of three measurements was taken for each index.

### 2.3. Heart specimen processing

After the experiments were completed, the mice were anesthetized with 10% chloral hydrate, and body weight (BW) was measured. Then, the thoracic cavity was cut open, the heart was removed, the residual blood was gently squeezed out of the heart cavity, and the heart weight (HW) was determined. Mouse heart tissue was divided into two parts for RNA retention and morphological staining.

### 2.4. Paraffin section preparation

Mouse ventricular myocardial tissue was fixed in 4% paraformaldehyde (Beijing Solarbio Science & Technology Co., Ltd., Beijing, China) for at least 24 h. After being rinsed with water, the tissues were dehydrated in an alcohol gradient (50%, 60%, 70%, 80%, 90%, 100%). The tissue was immersed in paraffin wax 3 times at 60 °C and cooled and solidified for slicing. Then, the tissues were cut into 5 μm-thick sections.

### 2.5. Hematoxylin-eosin (HE) staining

First, the sections were dewaxed. Afterward, the sections were soaked in hematoxylin (Beijing Solarbio Science & Technology Co., Ltd., Beijing, China) for approximately 5 min and stained with eosin (Beijing Solarbio Science & Technology Co., Ltd., Beijing, China) for 3 min. The sections were dehydrated in an increasing gradient of alcohol (70%, 80%, 90%, 95%, 100%) and xylene (Beijing Solarbio Science & Technology Co., Ltd., Beijing, China), cleared, and subsequently sealed with neutral gum (Beijing Solarbio Science & Technology Co., Ltd., Beijing, China) for preservation.

### 2.6. RT–PCR

In each group of mice, 100 mg of myocardial tissue was taken, and total RNA was extracted according to the instructions of the TRIZOL Reagent Extraction Kit (Tarkara, Japan), after which the RNA was dried at room temperature and fully dissolved by adding an appropriate amount of DEPC water (Tarkara, Japan). RNA concentration and purity (OD260/OD280 of 1.8–2.0 was considered pure RNA) were determined by a NanoDrop2000 (Thermo Fisher Scientific, Inc.). For each sample, 2 μg of RNA was reverse transcribed into cDNA using random primers and reverse transcriptase (Tarkara, Japan), and qRT−PCR was performed with the appropriate amount of reverse transcribed cDNA as template with specific primers. The reaction system contained 4 μl of cDNA template, 5 μl of SYBR-Green Mix (Tarkara, Japan), and 0.5 μl each of forward and reverse primers, and the program was as follows: 2 min at 94 °C predenaturation, 20 s at 94 °C, 30 s at 60 °C, and 30 s at 72 °C, for a total of 30 cycles. The results were calculated by the $2^{-\Delta\Delta CT}$ formula to determine the relative expression of the target mRNA in the experimental group compared with that in the control group.

### 2.7. JC-1 fluorescent probe to detect mitochondrial membrane potential (MMP)

After routine digestion of primary cardiomyocytes, the cells were inoculated in 20 $mm^2$ laser confocal dishes (Thermo Fisher Scientific, Inc., USA), treated according as indicated for 24 h and washed twice with PBS. Then, DMEM culture medium with 10 μg/ml JC-1 fluorescent probe was added in the dark, and the dye was washed off with PBS. The treated cells were placed on the laser confocal microscope loading stage, and the JC-1 fluorescent probe produced red fluorescence at an excitation wavelength of 585 nm and emission wavelength of 590 nm when the MMP was normal and green fluorescence at an excitation wavelength of 514 nm and emission wavelength of 529 nm when the MMP was reduced.

### 2.8. Immunohistochemistry (IHC)

Paraffin sections were dewaxed with xylene, hydrated in gradient alcohol and soaked in distilled water for 5 min. The sections were soaked in 0.01 M PBS (pH = 7.4) three times for 5 min each. Then, 50 μl of peroxidase blocker (Beijing Solarbio Science & Technology Co., Ltd., Beijing, China) was added to block endogenous peroxidase activity and incubated for 10 min at room temperature. Citrate antigen repair solution (CB, 0.01 M, pH 6.0, Beijing Solarbio Science & Technology Co., Ltd., Beijing, China) was used for antigen repair for 10 min, and 50 μl of normal goat serum (Beijing Solarbio Science & Technology Co., Ltd., Beijing, China) was added to each section and incubated for 30 min at room temperature. After that, the excess liquid was aspirated, and 50 μl of primary antibodies against GPX4 (59735, CST) or 4-hydroxynonenal (4-HNE) (ab48506, Abcam) was added to each section and incubated at 37 °C for 60 min. Then, 50 μl of biotin-labeled secondary antibody (Beijing Solarbio Science & Technology Co., Ltd., Beijing, China) was added to each section and incubated at 37 °C for 30 min. After that, 50 μl of biotin/horseradish peroxidase (HRP)-labeled chain affinity solution (Beijing Solarbio Science & Technology Co., Ltd., Beijing, China) was added to each section and incubated at 37 °C for 30 min. Then, 100 μl of freshly prepared DAB working solution (Beijing Solarbio Science & Technology Co., Ltd., Beijing, China) was added to each section and observed under the microscope for 15 min until positive staining was properly terminated. The slides were sensed with tap water, stained with hematoxylin, dehydrated in gradient alcohol, cleared with xylene, and sealed with neutral gum as described above.

### 2.9. Wheat Germ Agglutinin (WGA) staining

The sections were dewaxed as previously described, incubated in WGA solution (Beijing Solarbio Science & Technology Co., Ltd., Beijing, China) for 2 h at 37 °C protected from the light, washed with PBS, sealed with neutral gum, and photographed under a fluorescence microscope at 20x and 40× magnification. The surface area of individual cardiomyocytes was determined by measuring the area of myocardial tissue and the total number of nuclei in the field of view with ImageJ 1.43b software. The surface area of individual myocardial cells ($mm^2$) = tissue area ($mm^2$)/total number of nuclei.

### 2.10. Observation of ultrastructural changes in the myocardium by transmission electron microscopy (TEM)

Mouse hearts were removed, and approximately 1 $mm^3$ of apical tissue was collected within 3 min and immediately placed in centrifuge tubes filled with 2.5% glutaraldehyde electron microscopy fixative and stored at 4 °C. The tissues were fixed in 1% osmium acid (Beijing Xinxing Bairui Techonoloby Co., Ltd., Beijing, China) for 2 h at room temperature in the dark, dehydrated at room temperature, osmotically embedded, polymerized, prepared into ultrathin sections (70 nm), stained and observed under a transmission electron microscope (HITACHI, HT7800). The ultrastructural images of cardiomyocytes were collected at different magnifications.

### 2.11. Isolation and culture of primary cardiomyocytes

The protective effect of Pae against AngII-induced cardiomyocyte hypertrophy was investigated at the cellular level by isolating and culturing primary cardiomyocytes as previously described [24]. Briefly, myocardial tissues were digested with 0.0625% trypsin (Sigma–Aldrich; Merck KGaA) at 37 °C with constant agitation for 5 min, and the digested cells were added to DMEM/high-sugar medium (HyClone; GE Healthcare Life Sciences) with 10% FBS (HyClone; GE Healthcare Life Sciences) after each digestion to terminate trypsin activity. After that, the collected cell suspensions were combined and centrifuged at 1000×*g* for 5 min. The cells were resuspended in DMEM/high-sugar medium containing 10% FBS and inoculated into 10 cm dishes at 37 °C with 2.5% $CO_2$ for 2 h. After differential apposition, the apposed cardiac fibroblasts were cultured in DMEM/high-sugar medium containing 10% FBS for 48 h. After 48 h, the nonadherent cardiomyocytes were directly inoculated into 12-well plates at a concentration of $5 \times 10^3$ cells/well and 6-well plates at a concentration of $1 \times 10^5$ cells/well, and the medium was changed after 48 h to observe the pulsation of cardiomyocytes.

In contrast to those in the control group, hypertrophy was induced in cells in the AngII group using DMEM/high sugar medium containing $10^{-6}$ M AngII (A9290, Beijing Solarbio Science & Technology Co., Ltd., Beijing, China). Cells in the Pae intervention group were pretreated with DMEM/high sugar medium containing 20 μM AngII for 90 min, and then the medium was replaced with DMEM/high sugar medium containing $10^{-6}$ M AngII and 20 μM Pae (SP8040, Beijing Solarbio Science & Technology Co., Ltd., Beijing, China).

### 2.12. Western blotting

First, 50 μg of lysate was mixed with 1/4 volume of loading buffer (200 mM Tris-HCl, pH 6.8, 400 mM DTT, 8% SDS, 40% glycerol, 0.4% bromophenolane), boiled for 10 min, and then loaded onto 12% SDS–PAGE gels. Then, the proteins were transferred onto a PVDF membrane at a constant voltage of 40 V in an ice bath for 2.5 h. The membrane was blocked with 5% milk for 2 h at room temperature. After the membranes were washed, rabbit anti-rat primary antibodies against GPX4 (59735, CST), xCT (98051, CST) and GAPDH (5174, CST) were added and incubated overnight at 4 °C, and then goat anti-rabbit IgG/HRP secondary antibodies (Beijing Solarbio Science & Technology Co., Ltd., Beijing, China) were added and incubated at room temperature for 2 h. After the membranes were washed, ECL Western Blotting Substrate (Beijing Solarbio Science & Technology Co., Ltd., Beijing, China) was used. GAPDH was used as an internal control. The images were collected by a gel imaging system and analyzed by measuring the grayscale value. Quantitative analysis was performed using UVP 7.0 software (UVP LLC, Upland, CA, USA). Relative protein expression was normalized to GAPDH. All experiments were repeated three times. ImageJ 1.43b software (National Institutes of Health, Bethesda, MD, USA) was used for densitometry analysis.

### 2.13. Detection of cell viability by the Cell Counting Kit-8 (CCK-8) method

i. Primary cardiomyocytes were inoculated into 96-well plates and incubated with 10 μl of CCK-8 solution in each well for 2–4 h. Cell viability was calculated by measuring the absorbance of each well at a wavelength of 450 nm using Thermo Fisher Multiskan FC Enzyme Markers (Thermo Fisher Scientific, Inc., USA). Cell viability (%) = (absorbance of experimental wells - absorbance of blank wells)/(absorbance of control wells - absorbance of blank wells) × 100%. The experiment was repeated three times.

### 2.14. Quantification of MDA, GSH and $Fe^{2+}$

The Micro Malondialdehyde (MDA) Assay Kit (Beijing Solarbio Science & Technology Co., Ltd., Beijing, China), Micro Reduced Glutathione (GSH) Assay Kit (Beijing Solarbio Science & Technology Co., Ltd., Beijing, China) and Iron Assay Kit (ab83366, abcam, Cambridge) were used to detect MDA, GSH and $Fe^{2+}$ levels in mouse heart tissues according to the instructions.

### 2.15. BODIPY 581/591 C11 fluorescence intensity assay

The fluorescent probe BODIPY 581/591 C11 (Thermo Fisher Scientific, Inc., USA) is strongly lipophilic. The red fluorescence (excitation/emission: 581/610 nm) of BODIPY 581/591 C11 in the nonoxidized state gradually decreased, and the green fluorescence gradually increased when free lipid reactive oxygen species (ROS) in the cell oxidized BODIPY 581/591 C11.

### 2.16. Flow cytometry

The cells were divided into the Con group, AngII group ($10^{-6}$ M), AngII + Pae group ($10^{-6}$ M + 20 μM), and AngII + Fer-1 group ($10^{-6}$ M + 1 μM). Primary cardiomyocytes in the logarithmic growth phase were digested with trypsin and inoculated in 6-well plates, and the medium was discarded after 12 h of attachment. After centrifugation, 500 μl of 1 × Binding Buffer (Baiaobolai Biothechenology Co., Beijing, China) was added, and the cells were resuspended in flow cytometry tubes. Five microliters of Annexin V-PE was added to each tube and incubated for 10 min, and then 5 μl of 7-AAD staining was added. The cells were mixed and protected from light for 15 min at room temperature and then analyzed on a flow cytometer. Cell death was determined by flow cytometry using a BD FACSCalibur system (BD Biosciences, Franklin Lakes, NJ, USA), and the data were analyzed using ModFit software version 4.1 (Verity Software House, Inc., Topsham, ME, USA).

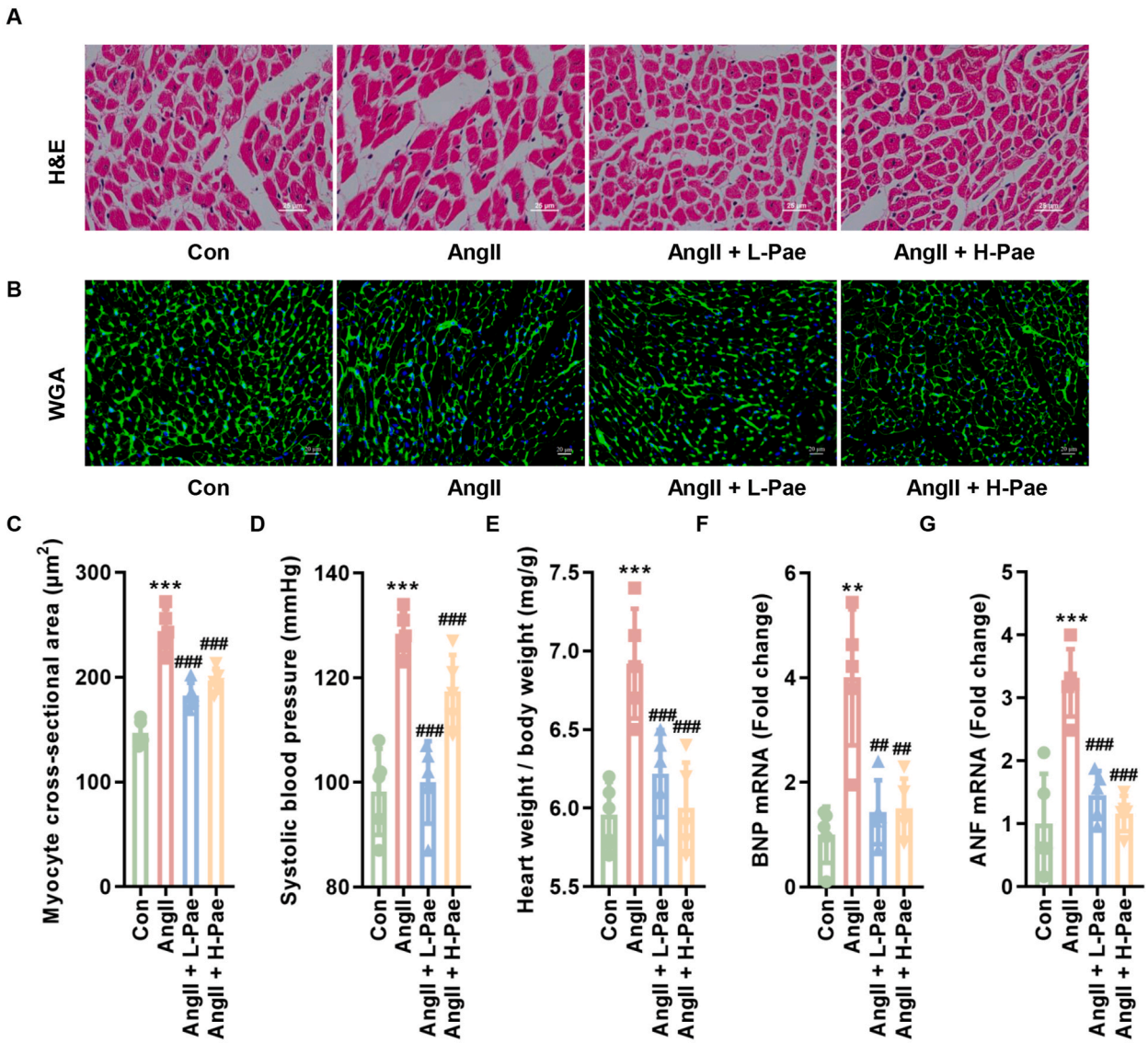


**Fig. 1.** Pae alleviated AngII-induced cardiac hypertrophy. (A) Representative H&E staining (bar represents 25 μm). (B) Representative WGA staining (bar represents 20 μm). (C) Statistical analysis of myocyte cross-sectional areas. L-Pae and H-Pae reduced systolic blood pressure (D) and the heart weight/body weight ratio (E) in AngII mice. The RT−PCR results showed that L-Pae and H-Pae treatment reduced the mRNA levels of BNP (F) and ANF (G) in AngII mice. n = 6 for each group; **p < 0.01, ***p < 0.001 vs. Con; ##p < 0.01, ###p < 0.001 vs. AngII. ANF: Natriuretic peptide A; AngII: angiotensin II; BNP: Natriuretic peptide B; Con: Control; H&E: Hematoxylin-eosin; H-Pae: High dose paeonol; L-Pae: Low dose paeonol; Pae: Paeonol; WGA: Wheat Germ Agglutinin.

### 2.17. FerroOrange staining

After the cells were treated, the medium was aspirated, and the cells were gently washed three times with prewarmed PBS. The cells were stained at 37 °C for 30 min, the medium was aspirated, and the cells were gently washed three times with prewarmed PBS and photographed using a confocal microscope (Olympus, Japan).

### 2.18. Statistical analysis

All experimental data are expressed as the mean ± standard deviation (mean ± SD), and SPSS 17.0 statistical software was used for statistical processing. Student's *t*-test was used for comparisons between two groups, and one-way ANOVA was used for comparisons between multiple groups. A value of $p < 0.05$ was considered statistically significant.

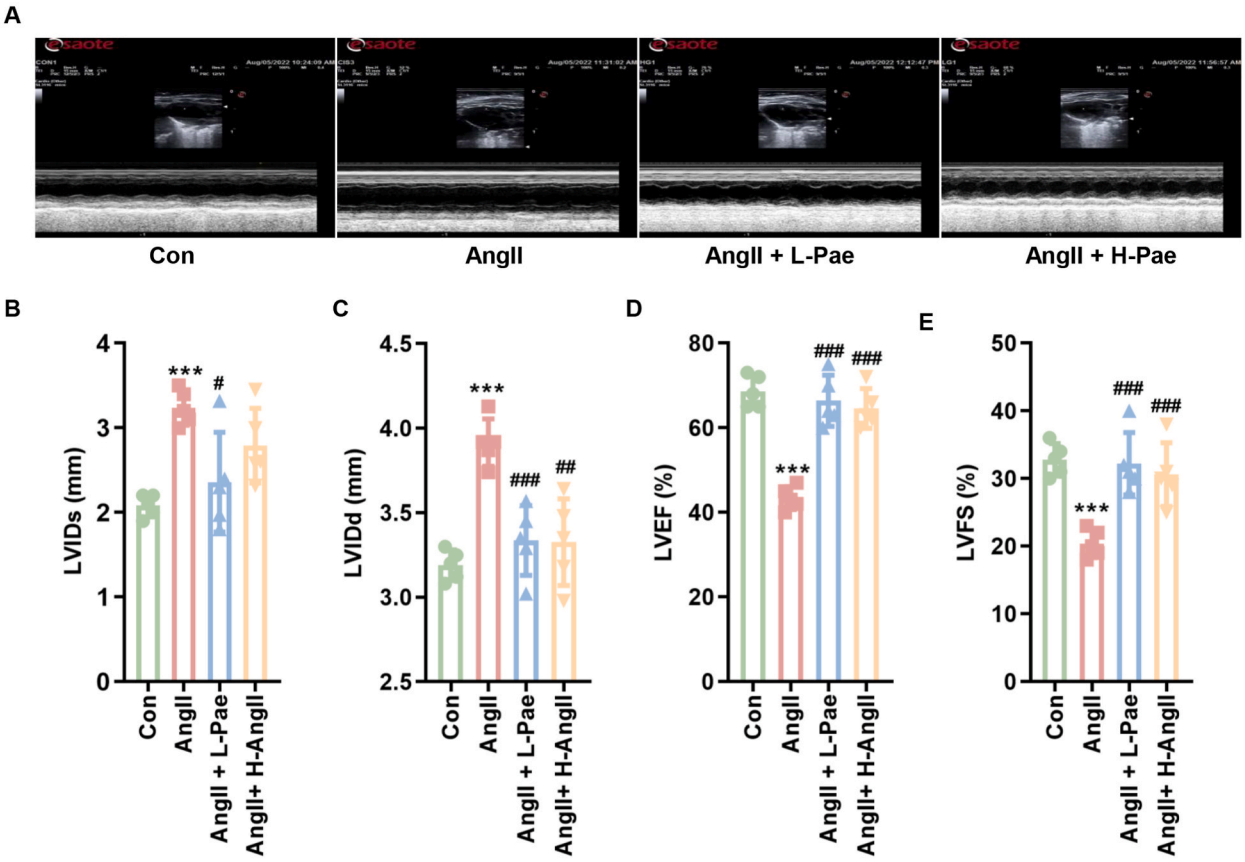


**Fig. 2.** Pae alleviates myocardial function in AngII mice. (A) Representative ECG images. LVIDs (B) and LVIDd (C) were significantly reduced, and LVEF (D) and LVFS (E) were significantly increased in the hearts of AngII mice after L-Pae and H-Pae treatment. n = 6 for each group; ***p < 0.001 vs. Con; ##p < 0.01, ###p < 0.001 vs. AngII. AngII: angiotensin II; ECG: Echocardiography; H-Pae: High dose paeonol; L-Pae: Low dose paeonol; LVEF: Left ventricular ejection fraction; LVFS: Left ventricular shortening. LVIDd: Left ventricular internal dimension at end diastole; LVIDs: Left ventricular posterior wall thickness at end systole.

## 3. Results

### 3.1. Pae ameliorated AngII-induced myocardial hypertrophy

To test whether AngII successfully induced hypertrophy in mouse myocardial tissue, we verified the effects of AngII on cardiac hypertrophy by H&E as well as WGA staining prior to Pae treatment. The results showed that AngII significantly induced cardiomyocyte hypertrophy (data not shown). Based on this, we further treated the Ang-myocardial hypertrophy mouse model with Pae. In control mice, the myocardium was neatly arranged, well structured and densely arranged, while the myocardial cells of AngII mice were hypertrophic and disorganized. The myocardial tissue was more densely arranged in the L-Pae and H-Pae groups than in the AngII group but was more disorganized than in the control group (Fig. 1A), and WGA staining showed that the myocardial cells were hypertrophied in the ANGII group compared with the control group (Fig. 1B). After treatment with L-Pae and H-Pae, cardiomyocyte hypertrophy was significantly improved (Fig. 1B and C). In the AngII group, cardiac systolic blood pressure was increased, while L-Pae and H-Pae decreased cardiac systolic blood pressure (Fig. 1D). Compared with those in the Con group, mice in the AngII group had a significant increase in heart weight/body weight (Fig. 1E). However, heart weight/body weight decreased significantly after L-Pae and H-Pae treatment (Fig. 1E). The RT−PCR results showed that AngII increased myocardial BNP and ANF mRNA levels, and the mRNA levels of BNP and ANF in myocardial tissue were reduced by L-Pae and H-Pae (Fig. 1F and G).

### 3.2. Pae improved myocardial function in AngII mice

Compared with those in the Con group, LVIDs and LVIDd were significantly higher and LVEF and LVFS were significantly lower in AngII mice (Fig. 2A, B, 2C, 2D and 2D). LVIDs and LVIDd were significantly lower, and LVEF and LVFS were significantly higher in the L-Pae and H-Pae groups than in the AngII group, and the changes in these indices were dose-dependent (Fig. 2A, B, 2C, 2D and 2E).

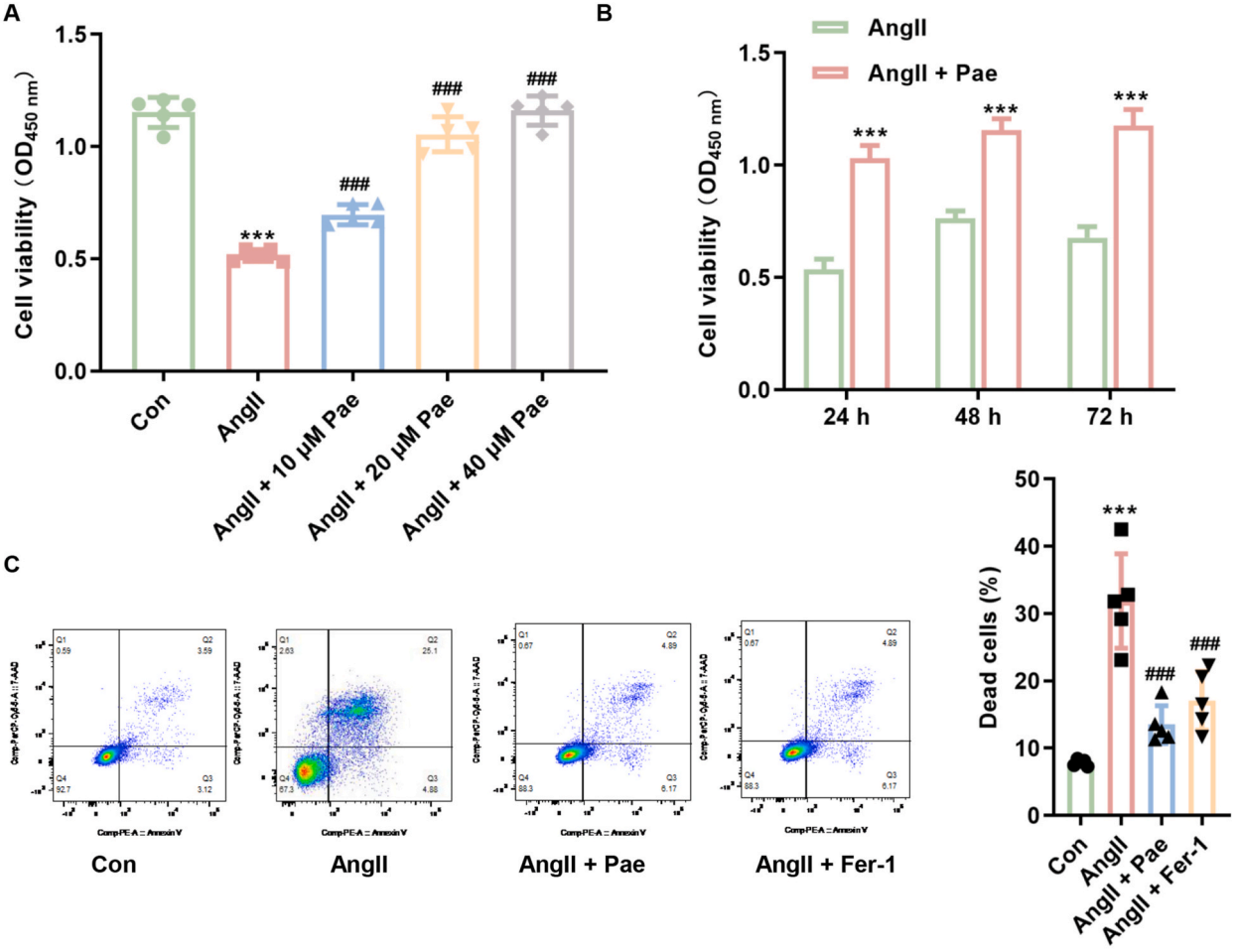


(caption on next page)

**Fig. 3.** Pae decreased AngII-induced death in primary cardiomyocytes. (A) The CCK-8 assay showed that pretreatment with 10 μM, 20 μM, and 40 μM Pae for 1 h effectively ameliorated the decrease in cell viability caused by Ang II. (B) The CCK-8 results showed that 20 μM Pae increased the viability of primary cardiomyocytes in a time- and gradient-dependent manner. (C) Flow cytometry revealed that Pae pretreatment effectively reduced AngII-induced cell death. (D) FerroOrange staining showed that Pae alleviated AngII-induced Fe2+ accumulation in primary cardiomyocytes. (E) C11 BODIPY 581/591 staining indicated that AngII-induced lipid ROS accumulation could be improved by Pae pretreatment. ***p < 0.001 vs. Con; ##p < 0.01, ###p < 0.001 vs. AngII. AngII: angiotensin II; CCK-8: Cell Counting Kit-8; Pae: Paeonol; ROS: Reactive oxygen species.

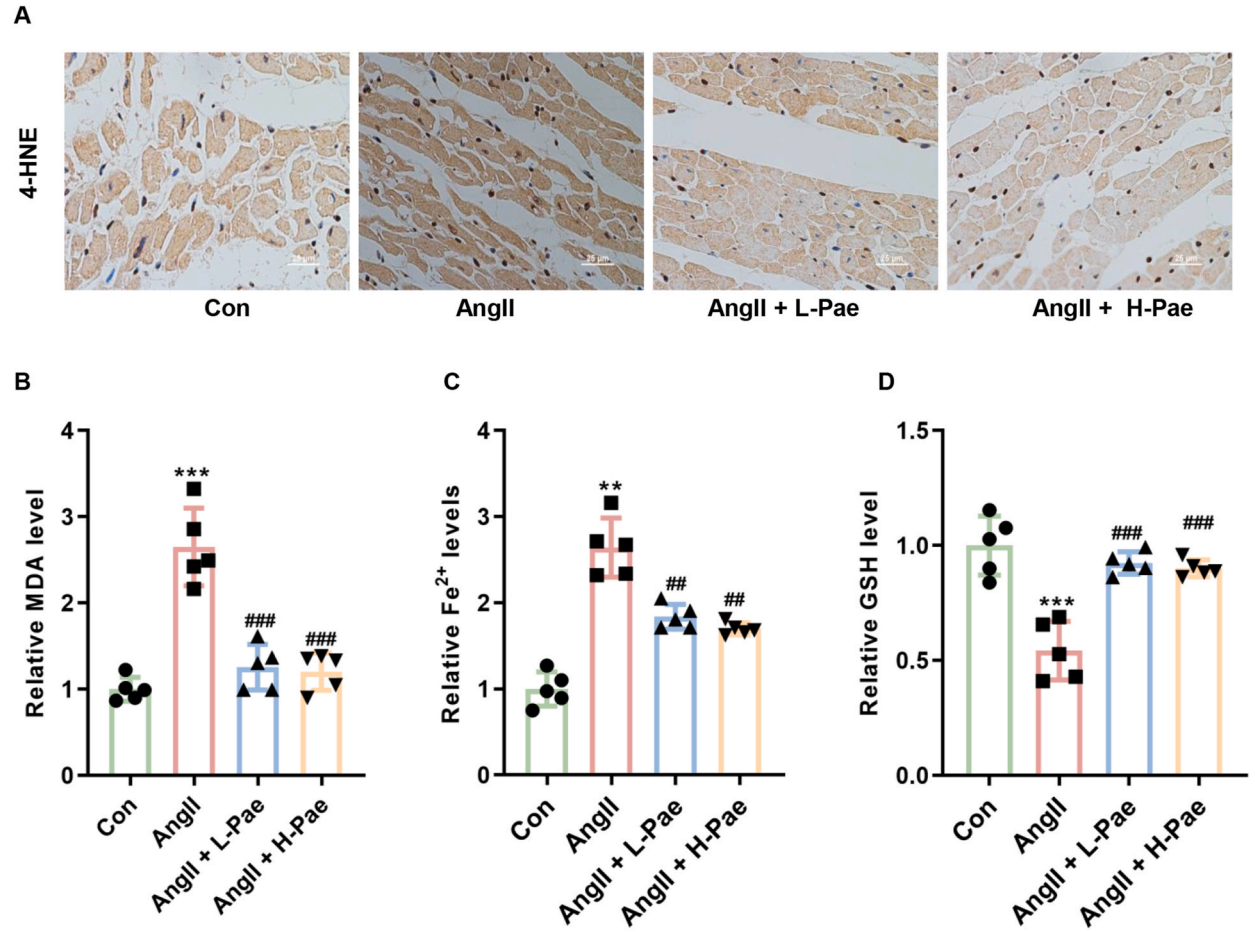


**Fig. 4.** Pae reduced AngII-induced lipid peroxidation and $Fe^{2+}$ accumulation in myocardial tissues. (A) IHC staining showed that the levels of 4-HNE were increased in the myocardial tissue of AngII-treated mice and were decreased after L-Pae and H-Pae treatment. The levels of MDA (B) and Fe2+ (C) were significantly increased in the myocardial tissues of mice in the AngII group, while the levels of MDA and Fe2+ were significantly decreased in the L-Pae and H-Pae groups. (D) The levels of GSH in the myocardial tissues of mice in the AngII group were decreased, while the levels of GSH in the L-Pae and H-Pae groups were increased. n = 6 for each group; **p < 0.01, ***p < 0.001 vs. Con; ##p < 0.01, ###p < 0.001 vs. AngII. 4-HNE: 4-Hydroxynonenal; AngII: angiotensin II; GSH: Glutathione; H-Pae: High dose paeonol; IHC: Immunohistochemistry; L-Pae: Low dose paeonol; MDA: Malondialdehyde.

### *3.3. Pae decreased AngII-induced death in primary cardiomyocytes*

Next, we examined whether Pae alleviated AngII-induced death in primary cardiomyocytes. As shown in Fig. 3A, AngII decreased primary cardiomyocyte viability in mice. Pretreatment with 10 μM, 20 μM, and 40 μM Pae for 1 h effectively ameliorated the decrease in cell viability caused by Ang II (Fig. 3A). In addition, we treated primary cardiomyocytes with 20 μM Pae for 24 h, 48 h, and 72 h. The CCK-8 results showed that 20 μM Pae increased the viability of primary cardiomyocytes in a time- and gradient-dependent manner (Fig. 3B). Flow cytometry revealed that AngII significantly increased the death of primary cardiomyocytes, while Pae pretreatment effectively reduced AngII-induced cell death (Fig. 3C). Interestingly, we found that a ferroptosis inhibitor (Fer-1) reversed AngII-induced cell death similarly to Pae (Fig. 3C). Therefore, we further examined whether Pae ameliorated AngII-induced ferroptosis. Our results revealed that AngII increased $Fe^{2+}$ and lipid ROS levels in primary cardiomyocytes, while Pae and Fer-1 pretreatment

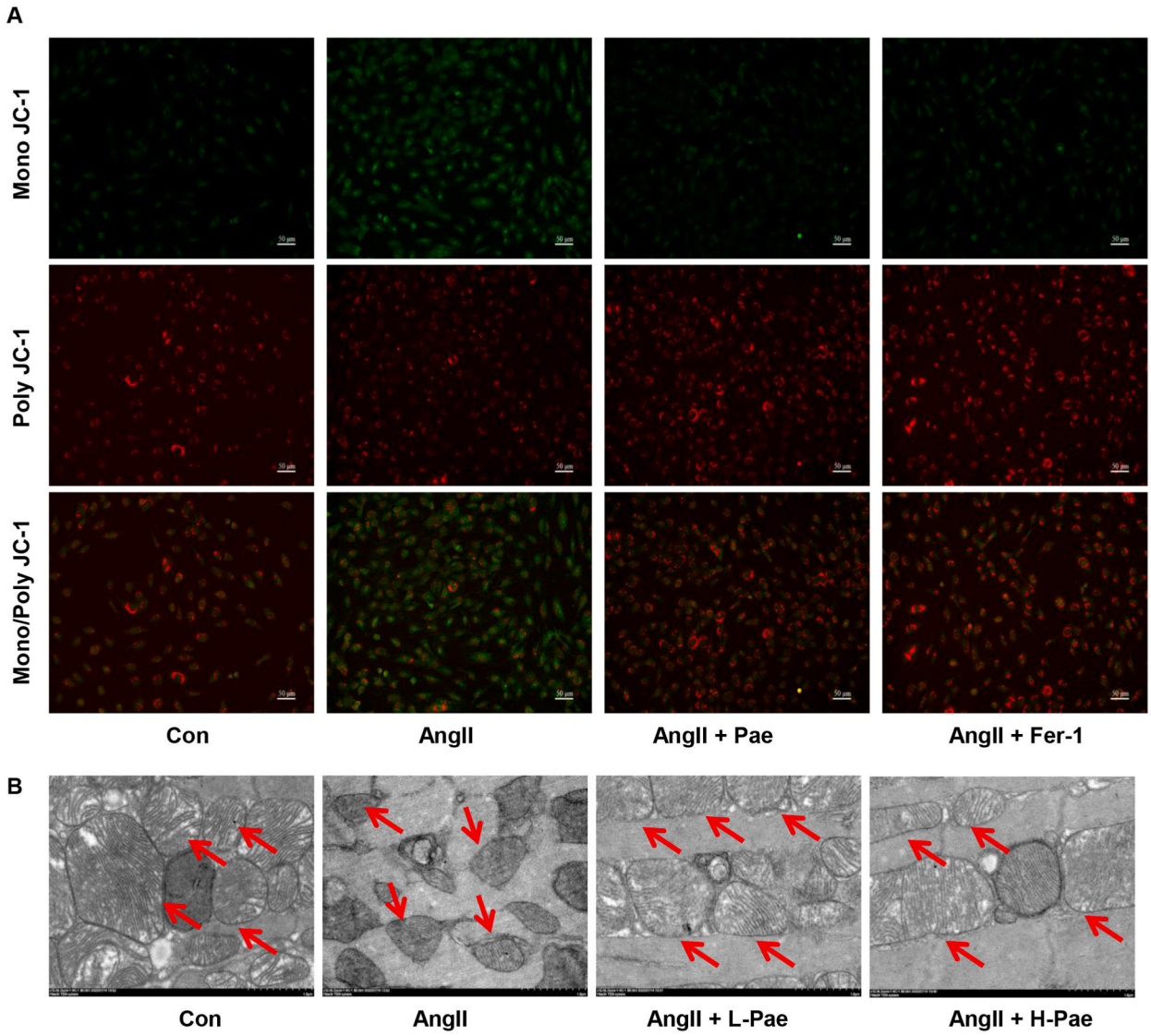


**Fig. 5.** Pae attenuated AngII-induced mitochondrial damage. (A) JC-1 staining showed that the AngII-induced decrease in mitochondrial membrane potential could be ameliorated by Pae (Bar represents 50 μm). (B) TEM analysis showed that L-Pae and H-Pae reduced the impairment of myocardial mitochondrial function in AngII mice (bar represents 1 μm). n = 6 for each group; AngII: angiotensin II; H-Pae: High dose paeonol; L-Pae: Low dose paeonol; TEM: Transmission electron microscopy.

effectively reversed $Fe^{2+}$ and lipid ROS accumulation (Fig. 3D and E). This result suggests that Pae can ameliorate AngII-induced ferroptosis in primary cardiomyocytes.

### *3.4. Pae reduced AngII-induced lipid peroxidation and $Fe^{2+}$ accumulation in myocardial tissues*

The levels of 4-HNE were increased in the myocardial tissue of AngII-treated mice and were decreased after L-Pae and H-Pae treatment (Fig. 4A). In addition, we examined the levels of MDA, Fe2+, and GSH in myocardial tissues. We found that the levels of MDA and Fe2+ were significantly increased in the myocardial tissues of mice in the AngII group, while the levels of MDA and Fe2+ were significantly decreased in the L-Pae and H-Pae groups and showed a dose-dependent change (Fig. 4B and C). In contrast, the levels of GSH in the myocardial tissues of mice in the AngII group were decreased, while the levels of GSH in the L-Pae and H-Pae groups were increased (Fig. 4D).

### *3.5. Pae attenuated AngII-induced mitochondrial damage*

Compared with the control, AngII increased green fluorescence and decreased red fluorescence, indicating a decrease in

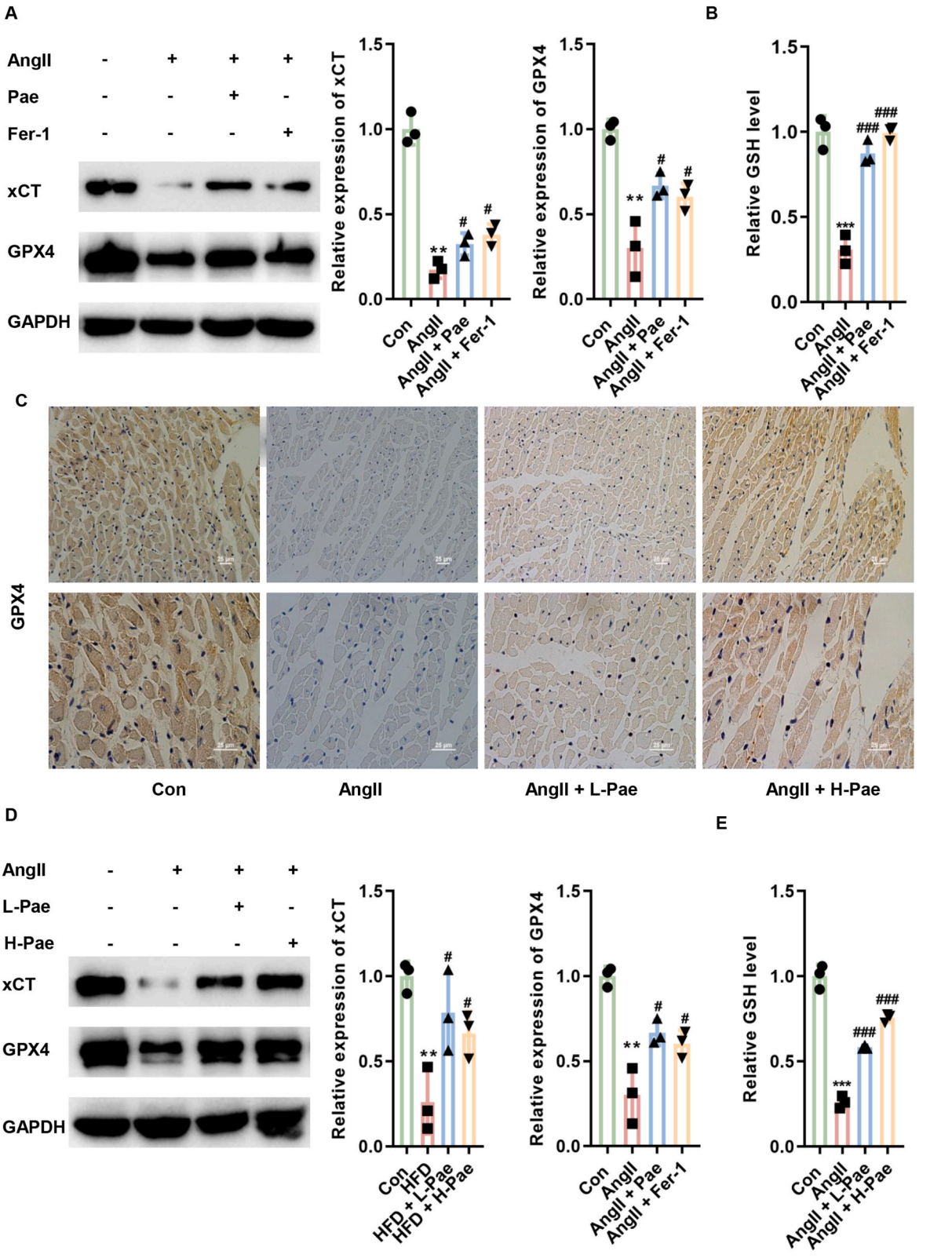


*(caption on next page)*

**Fig. 6.** Pae reversed the AngII-induced downregulation of the xCT-GSH-GPX4 axis in cardiac myocardial tissue. (A) In primary cardiomyocytes, the AngII-induced downregulation of xCT and GPX4 could be reversed by Pae (the uncropped versions were included in s.Fig. 6A-xCT, s.Fig. 6A-GPX4 and s.Fig. 6A-GAPDH). (B) AngII-induced GSH downregulation could be alleviated by Pae in primary cardiomyocytes. (C) IHC staining showed that L-Pae and H-Pae could reverse the AngII-induced decrease in GSH levels. (D) L-Pae and H-Pae restored the expression of xCT and GPX4 in the myocardial tissues of AngII-group mice to some extent (the uncropped versions were included in s.Fig. 6D-xCT, s.Fig. 6D-GPX4 and s.Fig. 6D-GAPDH). (E) The AngII-induced decrease in GSH in myocardial tissue could be ameliorated by L-Pae and H-Pae. n = 6 for each group; **p < 0.01, ***p < 0.001 vs. Con; ##p < 0.01, ###p < 0.001 vs. AngII. AngII: angiotensin II; GSH: Glutathione; GPX4: Glutathione peroxidase 4; H-Pae: High dose paeonol; IHC: Immunohistochemistry; L-Pae: Low dose paeonol; xCT: solute carrier family 7 member 11.

mitochondrial membrane potential (Fig. 5A). When primary cardiomyocytes were pretreated with Pae and Fer-1, red fluorescence was enhanced, and green fluorescence was diminished, indicating that the mitochondrial membrane potential was restored (Fig. 5A). In the con group, the mitochondria were larger in size, with intact outer membranes and abundant cristae (Fig. 5B). In contrast, in the ANGII group, the mitochondria were smaller, some of the cristae were reduced, and the outer membrane was lost (Fig. 5B). In comparison, after L-Pae and H-Pae treatment, the mitochondria were regularly arranged and increased in size, with more cristae and an intact mitochondrial outer membrane (Fig. 5B).

### *3.6. Pae enhanced the xCT-GPX4 axis and thereby alleviated AngII-induced ferroptosis in cardiomyocytes*

The xCT-GSH-GPX4 axis plays a major protective role against ferroptosis [25]. Therefore, we examined the effect of Pae on xCT-GSH-GPX4 expression in cardiomyocytes. As shown in Fig. 6A, AngII reduced the expression of xCT and GPX4 in primary cardiomyocytes, while Pae or Fer-1 restored the levels of xCT and GPX4 in cardiomyocytes. Moreover, AngII reduced the level of GSH in primary cardiomyocytes, while Pae or Fer-1 reversed the level of GSH to some extent (Fig. 6B). IHC staining showed that AngII reduced the expression of GPX4 in myocardial tissue, while the change in GPX4 expression in myocardial tissue was reversed in the L-Pae and H-Pae groups (Fig. 6C). Similar to the IHC results, AngII treatment downregulated xCT and GPX4 expression in myocardial tissues, but L-Pae and H-Pae restored xCT and GPX4 expression in myocardial tissues (Fig. 6D). AngII also decreased GSH levels in myocardial tissue compared with the control, whereas L-Pae and H-Pae significantly increased GSH levels in myocardial tissue (Fig. 6E).

## 4. Discussion

In this study, we investigated whether Pae alleviated AngII-induced cardiac remodeling. We demonstrated that Pae alleviated AngII-induced hypertrophy by inhibiting the activation of the xCT/GPX4 pathway and reducing the occurrence of ferroptosis in cardiomyocytes, thereby exerting a protective effect in vivo and in vitro.

Myocardial hypertrophy is characterized by an increase in myocardial cell surface area, and compensatory myocardial hypertrophy occurs in the heart to maintain normal cardiac function in response to various pathophysiological factors [26]. However, if abnormal pathological stimuli persist, such as hypertension, aortic stenosis, and aortic constriction, myocardial hypertrophy shifts from compensatory to decompensated, eventually leading to heart failure, arrhythmias and even sudden cardiac death [27,28]. Pae is extracted from natural plants and has antitumor and anti-inflammatory effects [9,29]. In the cardiovascular system, Pae has been shown to improve vascular atherosclerosis [9]. However, it is not clear whether Pae can alleviate AngII-induced myocardial hypertrophy. To test whether AngII successfully induced hypertrophy in mouse myocardial tissue, we verified the effect of AngII by H&E as well as WGA staining prior to Pae treatment. The results showed that AngII significantly induced cardiomyocyte hypertrophy (data not shown). Based on this, we treated the Ang-myocardial hypertrophy mouse model with Pae. Our data showedthat AngII induced significant myocardial hypertrophy (increased cardiomyocyte areas and upregulated ANP/BNP mRNA levels), while Pae significantly inhibited myocardial hypertrophy.

Ferroptosis is one of the pathological factors leading to myocardial infarction [9,30]. Normally, iron is in equilibrium in the body and is present in the circulatory system bound to transferrin [31]. However, when iron overload or equilibrium is disrupted, excess iron enters the cell and converts $Fe^{2+}$ to $Fe^{3+}$ through the Fenton or Fenton-like reactions and catalyzes the excessive production of ROS such as hydroxyl radicals [32]. Subsequently, $Fe^{3+}$ and ROS activate lipoxygenases that damage the cell membrane, causing changes in cellular morphology, such as membrane rupture, mitochondrial volume reduction, and mitochondrial cristae reduction or even disappearance [33,34]. In this study, ferroptosis was observed in the myocardium of AngII mice, GSH levels decreased, and ROS, MDA and iron ion levels increased, indicating that ferroptosis was involved in AngII-induced cell death. Pae could effectively abrogate excessive ROS accumulation and improve myocardial oxidative damage induced by AngII. In this study, we found that Pae significantly improved cell morphology, increased GSH levels and decreased ROS, MDA, and $Fe^{2+}$ levels in AngII mice, indicating that Pae could reduce lipid peroxidation and iron accumulation in the myocardium.

xCT is the light chain subunit of System Xc-, which is responsible for the reduction of cystine to cysteine and is involved in the synthesis of GSH [35,36]. It has been shown that inhibiting xCT leads to GSH depletion in the major intracellular antioxidant damage system, which in turn inhibits GPX4 activity, destabilizes intracellular redox and ROS accumulation, and is a marker of ferroptosis [37,38]. The results of this study showed that AngII significantly downregulated xCT expression in cardiomyocytes, decreased GSH levels, downregulated GPX4 expression and induced ROS accumulation. In contrast, Pae could inhibit AngII-induced ROS accumulation in cardiomyocytes and ameliorate the reduction in GSH levels and the downregulation of xCT and GPX4 expression caused by AngII.

However, there are limitations in the current study. First, myocardial hypertrophy can occur in the development of various cardiovascular diseases, such as hypertension, myocardial ischemia, hypertrophic cardiomyopathy, and ultimately progress to

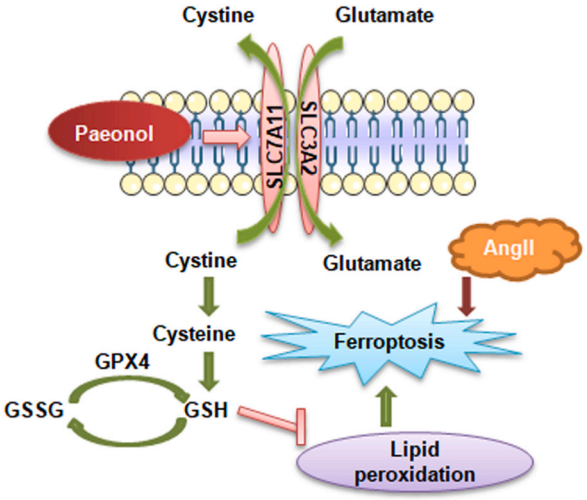


**Fig. 7.** Schematic of the mechanism by which paeonol improves AngII-induced cardiac hypertrophy by suppressing ferroptosis. AngII: angiotensin II.

myocardial fibrosis, impaired myocardial contractile function, and heart failure [39]. Hence, it is interesting to explore whether Pae prevented fibrosis in heart sections. In the future, we will explore whether Pae prevented fibrosis and the underlying mechanisms. Second, there are two main groups of antioxidant systems in the body. One group is antioxidant enzymes, including SOD, catalase (CAT), GPX4 and glutathione reductase (GR); the other group is non-enzymatic antioxidants, including GSH [40,41]. Since GSH works close to the enzymes GSH reductase and peroxidase, we evaluated their expression after Pae treatment in the AngII-induced cardiac injury mice. The results of this study showed that the levels of GPX4 and GSH were reduced by AngII, while Pae treatment reversed the levels of GPX4 and GSH. In the future, the effect of Pae on GR and CAT expression deserves further investigation. In addition, we mainly tested the therapeutic effect of Pae on AngII-induced cardiac hypertrophy. Therefore, we did not treat mice with Pae from a prevention perspective on the first day of AngII treatment. In a future study, we will started Pae treatment from the first day they started infusing AngII in mice.

## 5. Conclusion

Cardiac hypertrophy is commonly associated with hypertensive heart disease. AngII is an important cardiac hypertrophy factor, which can increase cardiomyocyte size. In this study, we found that Pae inhibited Ang II-induced cardiomyocyte hypertrophy, and its mechanism may be related to the activation of the xCT/GPX4 pathway, which inhibits ferroptosis (Fig. 7). In summary, for the first time, we discovered the protective effect of Pae on cardiomyocyte hypertrophy from the perspective of ferroptosis, which enriches the mechanistic study of Pae as a cardioprotective agent.

## Author contribution statement

Canzhang Liu: Performed the experiments; Analyzed and interpreted the data; Wrote the paper; Contributed reagents, materials, analysis tools or data. </p>

Shuipeng Liu: Conceived and designed the experiments; Analyzed and interpreted the data; Wrote the paper; Contributed reagents, materials, analysis tools or data. </p>

Xin Yi, Jie Yan, Qiang Liu, Teng Cao: Contributed reagents, materials, analysis tools or data. </p>

## Data availability statement

Data will be made available on request.

## Funding statement

This study was supported by grants (B2018056) from the Doctor Initial Fund of North China University of Science and Technology and Hebei Provincial Medical Science Research Project Program (Project code: 20231252).

## Declaration of competing interest

The authors declare that they have no known competing financial interests or personal relationships that could have appeared to

influence the work reported in this paper.

## Appendix A. Supplementary data

Supplementary data to this article can be found online at https://doi.org/10.1016/j.heliyon.2023.e19149.

## References


[1] L. Ba, J. Gao, Y. Chen, H. Qi, C. Dong, H. Pan, et al., Allicin attenuates pathological cardiac hypertrophy by inhibiting autophagy via activation of PI3K/Akt/mTOR and MAPK/ERK/mTOR signaling pathways, Phytomedicine 58 (2019), 152765.
[2] S. Iravanian, S.C. Dudley Jr., The renin-angiotensin-aldosterone system (RAAS) and cardiac arrhythmias, Heart Rhythm 5 (2008) S12–S17.
[3] E.E. Essick, F. Sam, Cardiac hypertrophy and fibrosis in the metabolic syndrome: a role for aldosterone and the mineralocorticoid receptor, Int. J. Hypertens. 2011 (2011), 346985.
[4] Y. Shen, X. Wang, R. Yuan, X. Pan, X. Yang, J. Cai, et al., Prostaglandin E1 attenuates AngII-induced cardiac hypertrophy via EP3 receptor activation and Netrin-1upregulation, J. Mol. Cell. Cardiol. 159 (2021) 91–104.
[5] C.L. Fan, S. Liang, M.N. Ye, W.J. Cai, M. Chen, Y.L. Hou, et al., Periplocymarin alleviates pathological cardiac hypertrophy via inhibiting the JAK2/STAT3 signalling pathway, J. Cell Mol. Med. 26 (2022) 2607–2619.
[6] Y. Yang, J. Du, R. Xu, Y. Shen, D. Yang, D. Li, et al., Melatonin alleviates angiotensin-II-induced cardiac hypertrophy via activating MICU1 pathway, Aging (Albany NY) 13 (2020) 493–515.
[7] Y. Li, Y. Shi, Y. He, X. Li, J. Yang, RNA binding Motif protein-38 regulates myocardial hypertrophy in LXR-alpha-dependent lipogenesis pathway, Bioengineered 12 (2021) 9655–9667.
[8] X. Fang, H. Wang, D. Han, E. Xie, X. Yang, J. Wei, et al., Ferroptosis as a target for protection against cardiomyopathy, Proc Natl Acad Sci U S A 116 (2019) 2672–2680.
[9] M. Wu, Z. Yu, X. Li, X. Zhang, S. Wang, S. Yang, et al., Paeonol for the treatment of atherosclerotic cardiovascular disease: a pharmacological and mechanistic overview, Front Cardiovasc Med 8 (2021), 690116.
[10] X. Chen, S. Xu, C. Zhao, B. Liu, Role of TLR4/NADPH oxidase 4 pathway in promoting cell death through autophagy and ferroptosis during heart failure, Biochem. Biophys. Res. Commun. 516 (2019) 37–43.
[11] X. Fang, Z. Cai, H. Wang, D. Han, Q. Cheng, P. Zhang, et al., Loss of cardiac ferritin H facilitates cardiomyopathy via slc7a11-mediated ferroptosis, Circ. Res. 127 (2020) 486–501.
[12] J.L. Parker, J.C. Deme, D. Kolokouris, G. Kuteyi, P.C. Biggin, S.M. Lea, et al., Molecular basis for redox control by the human cystine/glutamate antiporter system xc, Nat. Commun. 12 (2021) 7147.
[13] W.S. Yang, B.R. Stockwell, Ferroptosis: death by lipid peroxidation, Trends Cell Biol. 26 (2016) 165–176.
[14] C. Wang, W. Yuan, A. Hu, J. Lin, Z. Xia, C.F. Yang, et al., Dexmedetomidine alleviated sepsis-induced myocardial ferroptosis and septic heart injury, Mol. Med. Rep. 22 (2020) 175–184.
[15] Y. Zhang, X. Ren, Y. Wang, D. Chen, L. Jiang, X. Li, et al., Targeting ferroptosis by polydopamine nanoparticles protects heart against ischemia/reperfusion injury, ACS Appl. Mater. Interfaces 13 (2021) 53671–53682.
[16] Q. Zhang, H. Qu, Y. Chen, X. Luo, C. Chen, B. Xiao, et al., Atorvastatin induces mitochondria-dependent ferroptosis via the modulation of nrf2-xCT/GPx4 Axis, Front. Cell Dev. Biol. 10 (2022), 806081.
[17] L. Zhang, D.C. Li, L.F. Liu, Paeonol: pharmacological effects and mechanisms of action, Int Immunopharmacol 72 (2019) 413–421.
[18] L. Lu, Y. Qin, C. Chen, X. Guo, Beneficial effects exerted by paeonol in the management of atherosclerosis, Oxid. Med. Cell. Longev. 2018 (2018), 1098617.
[19] S. Chen, K. Luo, S. Bian, J. Chen, R. Qiu, X. Wu, et al., Paeonol ameliorates abdominal aortic aneurysm progression by the NF-kappaB pathway, Ann. Vasc. Surg. 77 (2021) 255–262.
[20] W. Yu, I. Ilyas, N. Aktar, S. Xu, A review on therapeutical potential of paeonol in atherosclerosis, Front. Pharmacol. 13 (2022), 950337.
[21] X. Wu, Y. Li, S. Zhang, X. Zhou, Ferroptosis as a novel therapeutic target for cardiovascular disease, Theranostics 11 (2021) 3052–3059.
[22] C. Chen, S. Liu, G. Cao, Y. Hu, R. Wang, M. Wu, et al., Cardioprotective effect of paeonol on chronic heart failure induced by doxorubicin via regulating the miR-21-5p/S-phase kinase-associated protein 2 Axis, Front Cardiovasc Med 9 (2022), 695004.
[23] X. Chen, Z. Zhang, X. Zhang, Z. Jia, J. Liu, X. Chen, et al., Paeonol attenuates heart failure induced by transverse aortic constriction via ERK1/2 signalling, Pharm. Biol. 60 (2022) 562–569.
[24] M. Akao, A. Ohler, B. O'Rourke, E. Marban, Mitochondrial ATP-sensitive potassium channels inhibit apoptosis induced by oxidative stress in cardiac cells, Circ. Res. 88 (2001) 1267–1275.
[25] Y. Yuan, L. Yucai, L. Lu, L. Hui, P. Yong, Y. Haiyang, Acrylamide induces ferroptosis in HSC-T6 cells by causing antioxidant imbalance of the XCT-GSH-GPX4 signaling and mitochondrial dysfunction, Toxicol. Lett. 368 (2022) 24–32.
[26] S. Yamamura, Y. Izumiya, S. Araki, T. Nakamura, Y. Kimura, S. Hanatani, et al., Cardiomyocyte sirt (sirtuin) 7 ameliorates stress-induced cardiac hypertrophy by interacting with and deacetylating GATA4, Hypertension 75 (2020) 98–108.
[27] Y. Chen, Y. Chang, N. Zhang, X. Guo, G. Sun, Y. Sun, Atorvastatin attenuates myocardial hypertrophy in spontaneously hypertensive rats via the C/EBPbeta/PGC-1alpha/UCP3 pathway, Cell. Physiol. Biochem. 46 (2018) 1009–1018.
[28] Y. Li, Y. Liang, Y. Zhu, Y. Zhang, Y. Bei, Noncoding RNAs in cardiac hypertrophy, J Cardiovasc Transl Res 11 (2018) 439–449.
[29] C. Liu, Y. Han, X. Gu, M. Li, Y. Du, N. Feng, et al., Paeonol promotes Opa1-mediated mitochondrial fusion via activating the CK2alpha-Stat3 pathway in diabetic cardiomyopathy, Redox Biol. 46 (2021), 102098.
[30] J. Li, F. Cao, H.L. Yin, Z.J. Huang, Z.T. Lin, N. Mao, et al., Ferroptosis: past, present and future, Cell Death Dis. 11 (2020) 88.
[31] X. Chen, R. Kang, G. Kroemer, D. Tang, Broadening horizons: the role of ferroptosis in cancer, Nat. Rev. Clin. Oncol. 18 (2021) 280–296.
[32] C. Liang, X. Zhang, M. Yang, X. Dong, Recent progress in ferroptosis inducers for cancer therapy, Adv Mater 31 (2019), e1904197.
[33] B. Hassannia, P. Vandenabeele, T. Vanden Berghe, Targeting ferroptosis to iron out cancer, Cancer Cell 35 (2019) 830–849.
[34] X. Chen, R. Kang, G. Kroemer, D. Tang, Ferroptosis in infection, inflammation, and immunity, J. Exp. Med. 218 (2021).
[35] R. Yi, H. Wang, C. Deng, X. Wang, L. Yao, W. Niu, et al., Dihydroartemisinin initiates ferroptosis in glioblastoma through GPX4 inhibition, Biosci. Rep. 40 (2020).
[36] B.Y. Fan, Y.L. Pang, W.X. Li, C.X. Zhao, Y. Zhang, X. Wang, et al., Liproxstatin-1 is an effective inhibitor of oligodendrocyte ferroptosis induced by inhibition of glutathione peroxidase 4, Neural Regen Res 16 (2021) 561–566.
[37] N. Lee, A.E. Carlisle, A. Peppers, S.J. Park, M.B. Doshi, M.E. Spears, et al., xCT-driven expression of GPX4 determines sensitivity of breast cancer cells to ferroptosis inducers, Antioxidants 10 (2021).
[38] Z. Zhang, J. Tang, J. Song, M. Xie, Y. Liu, Z. Dong, et al., Elabela alleviates ferroptosis, myocardial remodeling, fibrosis and heart dysfunction in hypertensive mice by modulating the IL-6/STAT3/GPX4 signaling, Free Radic. Biol. Med. 181 (2022) 130–142.

[39] M.A. McLellan, D.A. Skelly, M.S.I. Dona, G.T. Squiers, G.E. Farrugia, T.L. Gaynor, et al., High-resolution transcriptomic profiling of the heart during chronic stress reveals cellular drivers of cardiac fibrosis and hypertrophy, Circulation 142 (2020) 1448–1463.
[40] L.D. Coles, P.J. Tuite, G. Oz, U.R. Mishra, R.V. Kartha, K.M. Sullivan, et al., Repeated-dose oral N-acetylcysteine in Parkinson's disease: pharmacokinetics and effect on brain glutathione and oxidative stress, J. Clin. Pharmacol. 58 (2018) 158–167.
[41] M.X. Zhao, J.L. Wen, L. Wang, X.P. Wang, T.S. Chen, Intracellular catalase activity instead of glutathione level dominates the resistance of cells to reactive oxygen species, Cell Stress Chaperones 24 (2019) 609–619.